Light-Start CRISPR-Cas12a Reaction with Caged crRNA Enables Rapid and Sensitive Nucleic Acid Detection

Angewandte Chemie International Edition · 2023 · 10.1002/anie.202300663

8
Check for updates
A Journal of the Gesellschaft Deutscher Chemiker
Angewandte
GDCh
Chemie
International Edition
Accepted Article
Title: Light-start CRISPR-Cas12a reaction with caged crRNA enables rapid and sensitive nucleic acid detection
Authors: Menglu Hu, Ruhan Liu, Zhiqiang Qiu, Feng Cao, Tian Tian, Yunxin Lu, Yongzhong Jiang, and Xiaoming Zhou
This manuscript has been accepted after peer review and appears as an Accepted Article online prior to editing, proofing, and formal publication of the final Version of Record (VoR). The VoR will be published online in Early View as soon as possible and may be different to this Accepted Article as a result of editing. Readers should obtain the VoR from the journal website shown below when it is published to ensure accuracy of information. The authors are responsible for the content of this Accepted Article.
To be cited as: Angew. Chem. Int. Ed. 2023, e202300663
Link to VoR: https://doi.org/10.1002/anie.202300663
Angewandte Chemie International Edition
10.1002/anie.202300663
WILEY-VCH
RESEARCH ARTICLE
Light-Start CRISPR-Cas12a Reaction with Caged crRNA Enables Rapid and Sensitive Nucleic Acid Detection
Menglu Hu[a], Ruhan Liu[a], Zhiqiang Qiu[a], Feng Cao[a], Tian Tian[a], Yunxin Lu[c], Yongzhong Jiang[d], and Xiaoming Zhou*[a,b]
[a] Menglu Hu, Ruhan Liu, Zhiqiang Qiu, Feng Cao, Tian Tian, Prof. Xiaoming Zhou School of Life Sciences South China Normal University Guangzhou 510631, China E-mail: zhouxm@scnu.edu.cn
[b] Prof. Xiaoming Zhou
MOE Key laboratory of Laser Life Science & Guangdong Provincial Key Laboratory of Laser Life Science, College of Bio-photonics, South China Normal University
Guangzhou 510631, China
[c] Dr. Yunxin Lu
State Key Laboratory of Oncology in South China, Collaborative Innovation Center for Cancer Medicine Sun Yat-sen University Cancer Center
Guangzhou 510060, China
[d] Dr. Yongzhong Jiang
Institute of Health Inspection and Testing
Hubei Provincial Center for Disease Control and Prevention (Hubei CDC)
Wuhan, Hubei, 430079, China
These authors contributed equally to this work.
*To whom correspondence should be addressed.
Supporting information for this article is given via a link at the end of the document.
Abstract: The clustered regularly interspaced short palindromic repeats (CRISPR) system is a promising

platform for nucleic acid detection. Regulating the CRISPR reaction would be extremely useful to improve the detection efficiency and speed of CRISPR diagnostic applications. Here, we have developed a light-start CRISPR-Cas12a reaction by employing caged CRISPR RNA (crRNA). When combined with recombine polymerase amplification, a robust photocontrolled one-pot assay is achieved. The photocontrolled one-pot assay is simpler and is 50-fold more sensitive than the conventional assay. This improved detection efficiency also facilitates the development of a faster CRISPR diagnostic method. The detection of clinical samples demonstrated that 10-20 min is sufficient for effective detection, which is much faster than the current gold-standard technique PCR. We expect this advance in CRISPR diagnostics to promote its widespread detection applications in biomedicine, agriculture, and food safety.

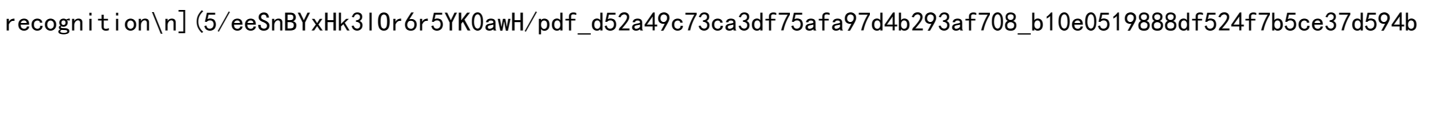
Introduction

The clustered regularly interspaced short palindromic repeats (CRISPR)‐Cas system is a young but promising bio-technology tool. The CRISPR‐Cas tool was originally developed for gene editing and has been rapidly developed for gene regulation, imaging, therapy, and most recently molecular diagnostic uses[11]. In particular, the outbreak of infectious diseases, such as Coronavirus Disease 2019 (COVID-19) and monkeypox, in recent years has triggered a serious public health crisis worldwide[21] At present, nucleic acid detection based on PCR technology is still a key means to control infectious diseases. However, it is particularly important to develop complementary or alternative technologies for PCR to meet the requirements of nucleic acid detection in noncentral laboratories and thus improve the prevention and controllability of infectious diseases[3]. Some unprecedented properties of CRISPR technology, such as guided RNA-mediated precise nucleic acid recognition, homogeneous reaction, and robust signal amplification mechanism, are extremely attractive for the development of next-generation nucleic acid detection technologies[4]. As a result, a number of CRISPR-based nucleic acid assays have been developed. Among these methods, technologies that combine isothermal nucleic acid amplification and CRISPR recognition, such as Specific High-Sensitivity Enzymatic Reporter UnLOCKing (SHERLOCK)[5], DNA endonuclease-targeted CRISPR trans reporter (DETECTOR)[6], and one-HOur Low-cost Multipurpose highly Efficient System (HOLMES)[7], are the most widely studied because they can be performed at a single reaction temperature and meet the sensitivity requirements of clinical detection.

Even so, these platform technologies still face a key bottleneck in their commercial application: the CRISPR cleavage reaction and nucleic acid amplification reaction are incompatible. When the isothermal amplification system is combined with the CRISPR reaction in a single tube, CRISPR cleavage will destroy the nucleic acid amplification template, thus compromising amplification efficiency and detection sensitivity. For that reason, in the original versions of SHERLOCK, DETECTOR, and HOLMES, nucleic acid amplification and CRISPR reactions were performed in separate tubes. However, the two-step reaction requires opening of the reaction tube and liquid transfer, which increases the complexity of the detection procedure. In addition, the liquid transfer step is highly susceptible to aerosol contamination, which can lead to false positives. Although a number of subsequent improvements have been developed, including the spatial isolation of reagents[8], the development of buffers or suboptimal protospacer adjacent motif (PAM) sites to

RESEARCH ARTICLE

a



b

1ef7508518051523035/tmp_zip_img/35cc4f93-1dc9-4853-9d75-188e589c3abb.png)
c
![<table><tr><td>Uncaged
crRNA</td><td>\n](5/eeSnBYxHk3lOr6r5YK0awH/pdf_d52a49c73ca3df75afa97d4b293af708_b10e0519888df524f7b5ce37d594b1ef7508518051523035/tmp_zip_img/6dc5caa9-b1ff-48a9-b4ee-7644f2a286f1.png)
d
![|时间|Vs (a.u. min)|\n|:---:|:---:|\n|0 s|0|\n|5 s|2000|\n|10 s|2000|\n|20 s|2750|\n|30 s|2750|\n|60 s|2750|\n|120
s|2250|\n|P|3500|\n|N|0|](5/eeSnBYxHk3lOr6r5YK0awH/pdf_d52a49c73ca3df75afa97d4b293af708_b10e0519888df524f7b5ce37d594b1ef7508518051523035/tmp_zip_img/8d8a0bd0-ef66-44bd-b12a-a3a61ead8940.png)
e
![|条件|P (a.u.)|N (a.u.)|\n|:---:|:---:|:---:|\n|Ambient light (8h) -|28000|500|\n|Ambient light (8h)
+|26000|500|\n|Avoid light (8 h) -|500|300|\n|Avoid light (8 h) +|500|400|\n|365 nm light (30 s)
+|26000|500|\n|365 nm light (30 s)
-|500|300|](5/eeSnBYxHk3lOr6r5YK0awH/pdf_d52a49c73ca3df75afa97d4b293af708_b10e0519888df524f7b5ce37d594b1ef7508518051523035/tmp_zip_img/31df410b-0331-479c-8b0e-aa97bb4d5506.png)
f
![|Template concentration (pM)|Uncaged crRNA|Caged
crRNA|\n|:---:|:---:|:---:|\n|100|43000|10000|\n|10|10000|6000|\n|1|100|300|\n|0.1|300|200|\n|NTC|150|120|
](5/eeSnBYxHk3lOr6r5YK0awH/pdf_d52a49c73ca3df75afa97d4b293af708_b10e0519888df524f7b5ce37d594b1ef7508518051523035/tmp_zip_img/04e874de-3401-4cbd-92e1-c4ad2a090463.png)
g
![|条件|P (a.u.)|N (a.u.)|\n|:---:|:---:|:---:|\n|1: Uncaged crRNA+, Caged crRNA-, Light+|35000|0|\n|2:
Uncaged crRNA-, Caged crRNA+, Light+|36000|0|\n|3: Uncaged crRNA-, Caged crRNA+, Light-|32000|0|\n|4:
Uncaged crRNA+, Caged crRNA-, Light+|32000|0|\n|5: Uncaged crRNA+, Caged crRNA+, Light+|32000|0|\n|6:
Uncaged crRNA-, Caged crRNA+, Light+|34000|0|\n|7: Uncaged crRNA-, Caged crRNA+, Light-|32000|0|\n|8:
Uncaged crRNA+, Caged crRNA+, Light+|32000|0|\n|9: Uncaged crRNA+, Caged crRNA+,
Light-|32000|0|](5/eeSnBYxHk3lOr6r5YK0awH/pdf_d52a49c73ca3df75afa97d4b293af708_b10e0519888df524f7b5ce37d594b1ef7508518051523035/tmp_zip_img/99dfb465-e1e5-46cd-a73d-1cd4f2997b53.png)
Figure 1. Development of light-start CRISPR-Cas12a reaction based on caged crRNA. (a) Structural diagram of the designed caged thymidine through the modification of NPOM. Decaging of thymidine can be achieved by UV light irradiation. (b) Light-start CRISPR-Cas12a reaction is designed by embedding caged thymidine into the crRNA of the Cas12a system. Caged thymidine of crRNA will disrupt the essential hydrogen bond for target DNA recognition and thus silence the activity of the Cas12a system. Rapid crRNA decaying can be achieved by UV light irradiation, thus allowing Cas12a activity restoration. (c) Evaluation of silencing and activity recovery efficiency of the caged crRNAs with varied numbers of NPOM modifications. The crRNA activity recovery efficiency was calculated by comparison with uncaged crRNA. (d) Evaluation of the required light irradiation time for CRISPR-Cas12a detection activity recovery. (e) Evaluating the stability of the caged crRNA after exposure to ambient light. The caged crRNA was pre-treated with ambient light or avoid light for 8 h at room temperature. Furthermore, the CRISPR-Cas12a reaction was irradiated with or without 365 nm UV light for 30 s. (f) Comparison of the nucleic acid detection efficiency of the CRISPR-Cas12a reaction using caged crRNA and uncaged crRNA. The Red and orange dashed lines correspond to the threshold lines for CRISPR-Cas12a reaction using caged crRNA and uncaged crRNA, respectively. And the threshold lines represent the detection limit, which was calculated from the mean plus 3 SDS of no-template control (NTC). (g) Evaluation of the universality of the NPOM modification strategy for constructing a light-start CRISPR-Cas12a reaction system. The crRNA activity recovery efficiency was calculated by comparison with uncaged crRNA. 1-3 represent EBV DNA-targeted crRNA1, MPXV DNA-targeted crRNA2, and the O-gene of SARS-CoV-2-targeted crRNA3, respectively. P represents the detection of the dsDNA target. N represents the blank control with RNase-free water as the target. Data are represented as

the mean ± standard error (n = 3 technical replicates). \Delta fluorescence (\Delta FL.) intensity represents the difference between the 60-min fluorescence value and the initial fluorescence value, a.u., arbitrary units. Vg represents the rate of reaction and was calculated according to the formula: Vg=\DeltaF/(T-1), where \DeltaF represents the difference between the 10-min fluorescence value and the initial fluorescence value, and T is the corresponding time frame.

weaken the CRISPR reaction[9], or the use of phase separation solutions[10], these methods remain inconvenient or suppress the efficiency of the CRISPR reaction, so the incompatibility problem is still not well solved.

Recently, we and others have developed a photocontrolled CRISPR technology to address this problem[11]. In this photocontrolled CRISPR assay, a silent oligonucleotide connected with a photocleavable linker (PC-linker) is designed to hybridize with the guide RNA to block the recognition and cleavage function of the CRISPR system. The photocontrolled

CRISPR assay separated the nucleic acid amplification and CRISPR reactions in the time dimension, realizing a closed, single-tube, high-sensitivity nucleic acid assay. Although photocontrolled CRISPR diagnostics are promising, the existing photocontrolled version still needs to be improved to facilitate their application. For example, the current method requires careful optimization of the ratio of PC-linker-containing oligonucleotides to guide RNA to achieve complete hybridization and silencing. This additional hybridization step complicates the assay process and the future construction of lyophilized reagents. In addition,

hybridization-based crRNA silencing strategy will prevent the prior binding of crRNA to Cas12a protein, thus affecting the Cas12a/crRNA stability. Accordingly, we sought to develop a more direct photocontrolled CRISPR assay to achieve simplified nucleic acid detection.

Here, we developed a new light-start CRISPR-Cas12 system using photochemically activated caged crRNA. In this technique, the caged crRNA prevents the Watson-Crick base pairing between crRNA and the target thus silencing the CRISPR-Cas12 activity. Rapid activity recovery can be achieved by photoinduced decaging. This developed light-start strategy could aid in the development of a robust one-pot CRISPR assay, which is simpler (using the same reagent preparation procedure as conventional CRISPR testing), faster (no RNA hybridization steps required), more stable (the caged crRNA does not affect its prior binding to Cas12a thus enhancing reagent stability), and more cost-effective (only a single caged crRNA is required), when compared to the previously developed photo-controlled CRISPR detection method.

Results and Discussion

Development of light-start CRISPR-Cas12a reaction based on caged crRNA.

It has previously been reported that modification of the caged group in the single-guide (sgRNA) of the Cas9 system can break the base pairing with the target nucleic acid, thereby silencing its nucleic acid recognition and cleavage function[12]. Cas9 activity is restored after the decaging of sgRNA by UV light, enabling the optical control of gene editing or regulation. Here, we embed 6-nitropiperonyloxymethyl-caged thymidine (NPOM-dt) into the crRNA (caged crRNA) of Lachnospiraceae bacterium ND2006 Cas12a (LbCas12a) to evaluate whether nucleic acid detection based on Cas12a can be designed with a light-start mode (Figure 1a and 1b). NPOM is modified in nitrogen heterocycles of thymidine and has been shown to be rapidly decaged with 365 nm UV light[13]. (Figure 1a). In this study, we first evaluated the feasibility of its photocontrol activity with an African swine fever virus (ASFV) DNA-targeted crRNA. Different numbers of NPOM-dt (2 to 6) were inserted into this crRNA, and their silencing effect and photomediated activity recovery efficiency were evaluated (Figure 1c). crRNA activity detection was based on LbCas12a trans-cleavage by a classical fluorescence method[6-7].

The results showed that weak crRNA activity could be detected with 2 NPOM-dt modifications, while no

activity could be detected with 3 - 6 NPOM-dt modifications, indicating that 3 NPOM-dt modifications were sufficient to destroy the base pairing between crRNA and target DNA (Figure 1c). We then performed the corresponding activity analysis in parallel when these crRNAs were exposed to UV light. The results showed that the activity of these crRNAs was restored to different degrees after decaging, among which the activity of 2 and 3 NPOM-modified crRNAs was restored to 109.6% and 90.2%, respectively, compared with that of uncaged crRNA (Figure 1c). Considering the silencing effect and activity recovery, we concluded that crRNA modified with 3 NPOMs was suitable for constructing light-start CRISPR-Cas12a for trans-cleavage and cis-cleavage reactions (Figure S1). Subsequently, the influence of the NPOM-dt modification positions on crRNA activity was also evaluated (Figure S2). The results showed that consecutive, terminal (two or more NPOM-dts modification at positions 16-20 in the spacer region) NPOM-dts modification at positions 16-20 in the spacer region) NPOM-dts modification at positions 16-20 in the spacer region) NPOM-dts modification at positions 16-20 in the spacer region) NPOM-dts modification at positions 16-20 in the spacer region) NPOM-dts modification at positions 16-20 in the spacer region) NPOM-dts modification at positions 16-20 in the spacer region) NPOM-dts modification at positions 16-20 in the spacer region) NPOM-dts modification at positions 16-20 in the spacer region) NPOM-dts modification at positions 16-20 in the spacer region) NPOM-dts modification at positions 16-20 in the spacer region) NPOM-dts modification at positions 16-20 in the spacer region) NPOM-dts modification at positions 16-20 in the spacer region) NPOM-dts modification at positions 16-20 in the spacer region) NPOM-dts m
dt modifications influenced the silencing and photoactivation efficiency of the crRNA. Discontinuous modification of three NPOM-dts at positions 1-15 of the crRNA in the spacer region achieved the most efficient silencing and photoactivation efficiency and is therefore highly recommended. We then tested the required light irradiation time with 365 nm light (35 W). The results show that 20-30 s is sufficient for NPOM decaging (Figure 1d). Notably, this caged crRNA was also shown to be sufficiently stable under natural light. We did not detect any activity recovery when it was placed under natural light for 8 h, indicating that the decaging of NPOM is wavelength selective (Figure 1e). We tested the nucleic acid detection efficiency of the developed light-start CRISPR-Cas12a reaction and compared it with uncaged crRNA. The results showed that the two kinds of crRNAs exhibited similar detection efficiency, although the caged crRNA caused a slight reduction in signaling intensity (Figure 1f). Finally, we wanted to know whether this NPOM-caged strategy was also applicable to other crRNAs. We evaluated crRNA1 targeting Epstein-Barr virus (EBV) DNA, crRNA2 targeting monkeypox virus (MPXV) DNA, and crRNA3 targeting the O-gene of severe acute respiratory syndrome coronavirus 2 (SARS-CoV-2) based on a similar three-NPOM-modified strategy. All three crRNAs showed excellent silencing effects and activity recovery efficiency (Figure 1g).

Development of photocontrolled one-pot recombinantas polymerase amplification (RPA)-CRISPR-Cas12a assayfor DNA detection.

Having completed the development of the light-start CRISPR-Cas12a reaction, we then evaluated its role in building a photocontrolled one-pot assay (Figure 2a). As has been discussed, nucleic acid amplification, such as RPA[14], can be severely disrupted by the CRISPR-Cas12a cleavage reaction if all the components are put into a single test tube. We expected that this problem could be solved by temporarily silencing the CRISPR-Cas12a reaction with caged crRNA. After nucleic acid amplification is completed, the CRISPR-Cas12a system was activated by light to ensure that both nucleic acid amplification and the CRISPR-Cas12a reaction were not affected, thus achieving highly sensitive nucleic acid detection (Figure 2a).

We then developed a photocontrolled one-pot assay using ASFV DNA-targeted crRNA. In a component-deletion assay, it was found that only UV light could mediate signal generation in the presence of all required components, indicating that the designed one-pot assay relied strictly on light irradiation initiation (Figure 2b). It was anticipated that the sensitivity of the one-pot assay would be enhanced by photoregulation of the Cas12a reaction. We then evaluated the assay efficiency of two parallel one-pot

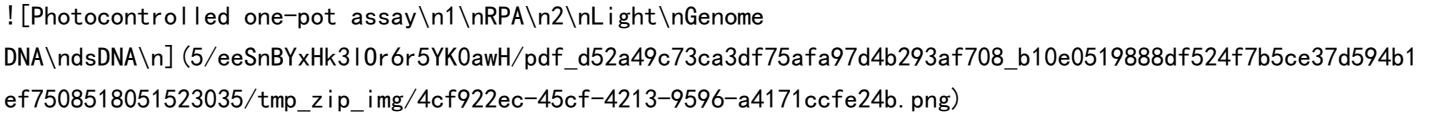
assays with caged crRNA and uncaged crRNA (Figure 2c and 2d). Using identical gradient-diluted ASFV DNA plasmids as templates, we found that the photocontrolled one-pot assay based on caged crRNA exhibited significant signal enhancement. In an unoptimized system, we observed a 50-fold increase in sensitivity (Figure 2c and 2d). In addition, it was considered that the photoactivation timing may have a key impact on the detection speed. As shown in Figure S3, photoactivation timing with 10, 20, and 30 min were set, and samples with final concentrations of 10^0 and 10^{-1 copies/L can be both effectively detected regardless of the photoactivation timing. When the photoactivation timing is set at 10 min, the signal-to-noise ratio of the low concentration samples is compromised. In general, adjusting the photoactivation timing seems to be useful for improving the

detection speed, especially when the sample concentration is relatively high.

We next evaluated the photocontrolled one-pot assay for the detection of clinical EBV-infected blood samples. EBV infections have been shown to be associated with multiple types of human cancers, including lymphocytic and epithelial cell carcinomas[15]. In particular, there is growing evidence that detection of EBVs can provide valuable information for the early diagnosis of undifferentiated nasopharyngeal carcinoma[16]. A recent study showed that the sensitivity and specificity of EBV DNA in nasopharyngeal cancer screening were 97.1% and 98.6%, respectively[16]. In this study, 14 clinical blood samples, including 10 EBV-positive samples and 4 EBV-negative samples, were collected, and identified by quantitative PCR (qPCR). The qPCR results showed that these positive samples were detected before 30 cycles because of the high EBV viral load (Figure S4). Running

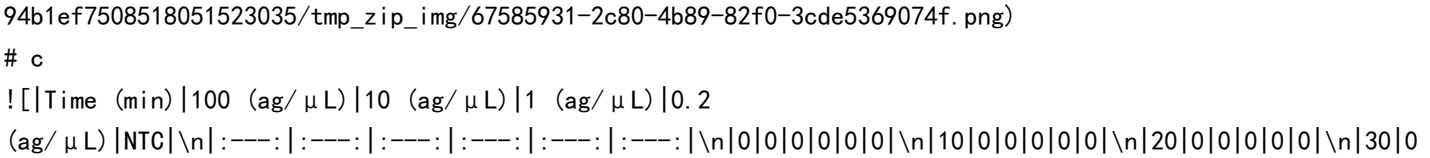
30 cycles takes approximately one hour in the PCR method. We then analyzed these samples using conventional and photocontrolled one-pot RPA-CRISPR/Cas12a assays. As shown in Figure 2e and 2f, all these samples can be effectively detected by these two methods. Both methods were able to detect all positive samples before 40 min, but the photocontrolled method achieved a significant signal-to-noise ratio improvement (Figure 2f). Considering the high detection efficiency of the photocontrolled method, we further evaluated whether this improvement could shorten the nucleic acid detection time. The results showed that high detection performance was still achieved when the light-mediated activation of Cas12a was set at 10 min after nucleic acid amplification (Figure 2g). All positive samples were effectively detected within 10 to 20 min, indicating that the photocontrolled method can significantly improve the detection sensitivity and speed (Figure 2g).

a



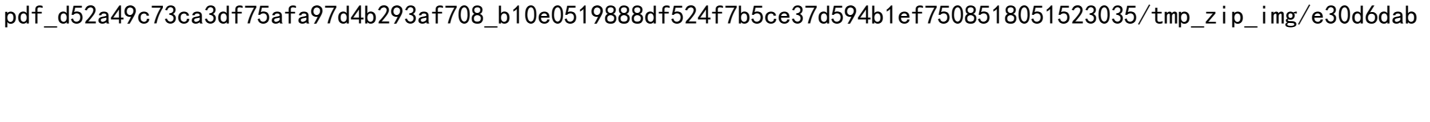
b

列	Primers	Rehydration buffer	MgOAc	Template	Cas12a components	RPA components	Light	FL intensity (a.u.)
1	-	-	-	-	+	+	-	500
2	-	-	-	-	+	+	+	500
3	-	-	+	-	+	+	-	500
4	-	-	+	-	+	+	+	500
5	-	+	+	+	+	+	-	500
6	-	+	+	+	+	+	+	1000
7	+	+	+	+	+	+	+	20000



c

Time (min)	100 (ag/μL)	10 (ag/μL)	1 (ag/μL)	0.2 (ag/μL)	NTC
0	0	0	0	0	0
10	0	0	0	0	0
20	0	0	0	0	0
30	0	0	0	0	0
40	25000	2500	500	250	0
50	45000	15000	2000	750	0
60	48000	25000	3000	1000	0
70	49000	30000	3500	1250	0
80	49000	35000	4000	1500	0
90	49000	38000	4500	1750	0



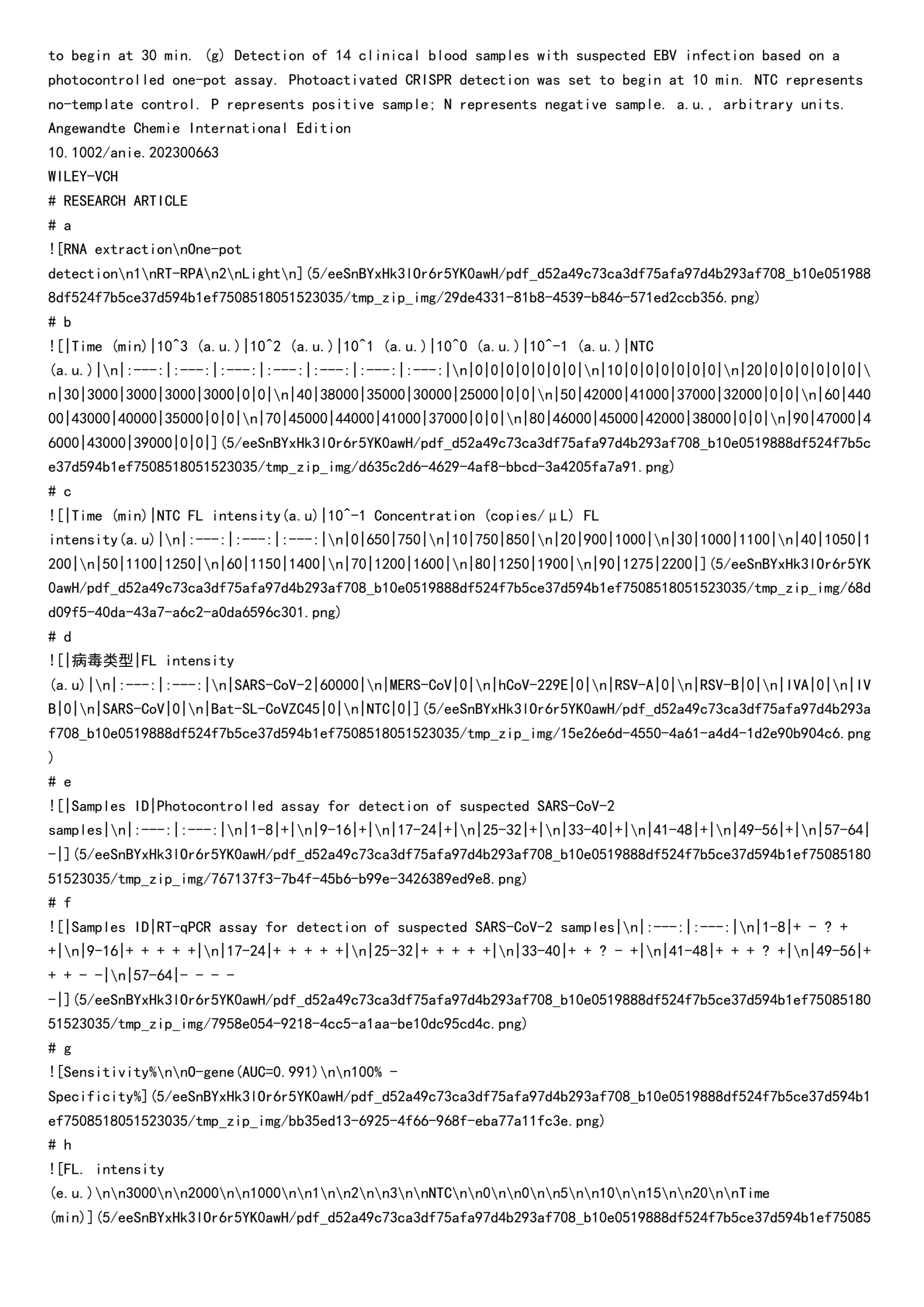
-a33d-433b-9db3-b22379f8f545.png)
d
![|Time (min)|Concentration (ag/μL) = 100|Concentration (ag/μL) = 10|Concentration (ag/μL) = 1|Concentration (ag/μL) = 0.2|NTC|\n|:---:|:---:|:---:|:---:|:---:|:---:|\n|0|0|0|0|0|0|\n|10|0|0|0|0|0|\n|20|0|0|0|0|0|\n|30|0|0|0|0|0|\n|40|1000|0|0|0|0|\n|50|3000|500|0|0|0|\n|60|7000|1000|500|0|0|\n|70|12000|2000|1000|0|0|\n|80|18000|4000|2000|0|0|\n|90|23000|7000|3000|0|0|](5/eeSnBYxHk3lOr6r5YK0awH/pdf_d52a49c73ca3df75afa97d4b293af708_b10e0519888df524f7b5ce37d594b1ef7508518051523035/tmp_zip_img/39fd38da-ff19-4d47-821e-524ab853be54.png)
e
![|Time (min)|P1|P2|P3|P4|P5|P6|P7|P8|P9|P10|N1|N2|N3|N4|\n|:---:|:---:|:---:|:---:|:---:|:---:|:---:|:---:|:---:|:---:|:---:|:---:|:---:|:---:|:---:|:---:|:---:|:---:|:---:|:---:|:---:|\n|0|0|0|0|0|0|0|0|0|0|0|0|0|0|0|0|\n|10|0|0|0|0|0|0|0|0|0|0|0|0|0|0|0|\n|20|0|0|0|0|0|0|0|5000|5000|5000|5000|5000|5000|\n|30|0|0|0|0|0|15000|0|0|20000|20000|20000|20000|20000|20000|\n|40|0|10000|10000|10000|10000|25000|0|0|30000|30000|30000|30000|30000|30000|\n|50|0|20000|20000|20000|20000|30000|0|0|35000|35000|35000|35000|35000|35000|\n|60|0|30000|30000|30000|30000|35000|0|0|38000|38000|38000|38000|38000|38000|\n|70|0|35000|35000|35000|35000|38000|0|0|40000|40000|40000|40000|40000|40000|\n|80|0|38000|38000|38000|38000|39000|0|0|42000|42000|42000|42000|42000|42000|\n|90|0|40000|40000|40000|40000|40000|0|0|45000|45000|45000|45000|45000|45000|](5/eeSnBYxHk3lOr6r5YK0awH/pdf_d52a49c73ca3df75afa97d4b293af708_b10e0519888df524f7b5ce37d594b1ef7508518051523035/tmp_zip_img/120e389b-76a1-4a00-beaf-b58731d7387c.png)
f
![FL. intensity (a. u.)\n\n20000\n\nP1 P9\n\nP2 P10\n\nP3 N1\n\nP4 N2\n\nP5 N3\n\nP6 N4\n\nP7\n\nP8\n\n0 10 20 30 40 50 60 70 80 90\n\nTime (min)](5/eeSnBYxHk3lOr6r5YK0awH/pdf_d52a49c73ca3df75afa97d4b293af708_b10e0519888df524f7b5ce37d594b1ef7508518051523035/tmp_zip_img/c0f004d6-a0bb-42d9-b8c5-773f20d5e6bd.png)
g
![|Time (min)|P1|P2|P3|P4|P5|P6|P7|P8|P9|P10|N1|N2|N3|N4|\n|:---:|:---:|:---:|:---:|:---:|:---:|:---:|:---:|:---:|:---:|:---:|:---:|:---:|:---:|:---:|:---:|:---:|:---:|:---:|:---:|:---:|\n|0|0|0|0|0|0|0|0|0|0|0|0|0|0|0|0|\n|10|0|0|0|0|0|0|0|0|0|0|0|0|0|0|0|\n|20|35000|35000|35000|35000|35000|30000|35000|0|40000|40000|40000|40000|40000|40000|\n|30|40000|42000|40000|38000|42000|35000|40000|0|43000|42000|41000|42000|41000|41000|\n|40|41000|43000|41000|39000|43000|36000|41000|0|43000|43000|42000|42000|42000|42000|\n|50|41000|43000|41000|39000|43000|36000|41000|0|43000|43000|42000|42000|42000|42000|\n|60|41000|43000|41000|39000|43000|36000|41000|0|43000|43000|42000|42000|42000|42000|\n|70|41000|43000|41000|39000|43000|36000|41000|0|43000|43000|42000|42000|42000|42000|\n|80|41000|43000|41000|39000|43000|36000|41000|0|43000|43000|42000|42000|42000|42000|\n|90|41000|43000|41000|39000|43000|36000|41000|0|43000|43000|42000|42000|42000|42000|](5/eeSnBYxHk3lOr6r5YK0awH/pdf_d52a49c73ca3df75afa97d4b293af708_b10e0519888df524f7b5ce37d594b1ef7508518051523035/tmp_zip_img/d9a2d5a8-4371-4b6e-860c-28f4ac1c1b7f.png)
Figure 2. Development of photocontrolled one-pot RPA-CRISPR-Cas12a assay for DNA detection. (a) The light-start CRISPR-Cas12a reaction was integrated with RPA to construct a fully closed one-pot DNA detection technique. In this single-tube reaction, RPA is first performed to produce DNA amplification products, followed by photoactivation of CRISPR-Cas12a and then initiation of nucleic acid detection. (b) Reaction component deletion experiments for demonstrating the photocontrolled one-pot RPA-CRISPR-Cas12a DNA assay concept. Data are represented as the mean ± standard error (n = 3 technical replicates). Sensitivity analysis of the photocontrolled one-pot RPA-CRISPR-Cas12a DNA assay (c) and the conventional one-pot RPA-CRISPR-Cas12a DNA assay (d). Data are represented as the mean ± standard error (n = 3 technical replicates). (e) Detection of 14 clinical blood samples with suspected EBV infection based on the conventional one-pot RPA-CRISPR-Cas12a DNA assay. (f) Detection of 14 clinical blood samples with suspected EBV infection based on a photocontrolled one-pot assay. Photoactivated CRISPR detection was set

to begin at 30 min. (g) Detection of 14 clinical blood samples with suspected EBV infection based on a photocontrolled one-pot assay. Photoactivated CRISPR detection was set to begin at 10 min. NTC represents no-template control. P represents positive sample; N represents negative sample. a.u., arbitrary units.

Angewandte Chemie International Edition
10.1002/anie.202300663
WILEY-VCH

RESEARCH ARTICLE

a



b

c

d

e

f

g

h

18051523035/tmp_zip_img/1a30f4f2-160e-4abf-ae77-b82349abda8d.png)
i
![FL intensity
(e.u.)\n\n2000\n\n1500\n\n1000\n\n500\n\n0\n\n10\n\n20\n\nCycles\n\n30\n\n40](5/eeSnBYxHk3lOr6r5YK0awH/pdf_d52a49c73ca3df75afa97d4b293af708_b10e0519888df524f7b5ce37d594b1ef7508518051523035/tmp_zip_img/106ee182-e1b1-4fc2-814a-9a23dbcae213.png)
Figure 3. Development of photocontrolled one-pot RT-RPA-CRISPR-Cas12a assay for SARS-CoV-2 RNA detection. (a) Light-start CRISPR-Cas12a reaction is integrated with RT-RPA to construct a one-pot SARS-CoV-2 RNA detection technique. In this single-tube reaction, RT-RPA is first performed to convert SARS-CoV-2 RNA amplification products, followed by photoactivation of CRISPR-Cas12a and then initiation of nucleic acid detection. (b) Evaluation of the detection sensitivity of the photocontrolled one-pot RT-RPA-CRISPR-Cas12a assay by analyzing SARS-CoV-2 RNA samples with gradient dilution. Data are represented as the mean ± standard error (n = 3 technical replicates). (c) An enlarged view of the curves at the detection of 101 copies/L SARS-CoV-2 RNA. (d) Evaluation of the detection specificity of the photocontrolled one-pot RT-RPA-CRISPR-Cas12a assay by analysis of SARS-CoV-2 RNA against other coronavirus and human respiratory viruses (middle east respiratory syndrome coronavirus (MERS-CoV), human coronavirus 229E (hCoV-229EE), respiratory syncytial virus type A (RSV-A), respiratory syncytial virus type B (RSV-B), influence A virus (IVA), influence B virus (IVB), SARS-CoV, and bat SARS-like coronavirus (bat-SL-CoVZC45)). Data are represented as the mean ± standard error (n = 3 technical replicates). (e) Detection of 64 clinical SARS-CoV-2 RNA samples by photocontrolled one-pot RT-RPA-CRISPR-Cas12a assay. + represents positive samples. - represents negative samples. The diagnostic results were determined by setting the photoactivation time at 30 min. (f) Detection of 64 clinical SARS-CoV-2 RNA samples by RT-aPCR. + represents positive samples. - represents negative samples. ? represents suspected samples (C; 38). (g) ROC curve analysis of the detection accuracy in clinical applications. Comparison of the required detection time of the photocontrolled CRISPR assay (h) and the RT-qPCR method (ii) based on the analysis of three clinical SARS-CoV-2 RNA samples with C values of approximately 35. Photoactivated CRISPR detection was set to begin at 10 min. NTC represents no-template control. a.u., arbitrary units.
Angewandte Chemie International Edition
10.1002/anie.202300663
WILEY-VCH
RESEARCH ARTICLE
Development of photocontrolled one-pot reverse-transcription RPA (RT-RPA)-CRISPR-Cas12a assay for SARS-CoV-2 RNA detection.
We hypothesized that the light-start CRISPR-Cas12a reaction should also facilitate the development of a highly sensitive one-pot RNA assay. We integrated RT-RPA and light-start CRISPR-Cas12a reaction into a single tube to detect clinical SARS-CoV-2 RNA samples. Although CRISPR-Cas12a does not directly degrade SARS-CoV-2 RNA samples, DNA converted from SARS-CoV-2 RNA via RT-RPA can be degraded by CRISPR-Cas12a, resulting in the loss of amplification templates and impaired detection efficiency. Therefore, activating CRISPR-Cas12a with light after amplification is complete will ensure that sufficient amplification products accumulate for detection (Figure 3a). The photocontrolled one-pot RNA assay was first employed to detect digital PCR-counted SARS-CoV-2 RNA based on an O-gene targeted caged crRNA. As shown in Figure 3b, as low as 1 copy per microliter of SARS-CoV-2 RNA samples was reliably detected within 30-40 min. Notably, a concentration of 0.1 copy per microliter of SARS-CoV-2 RNA samples (equal to 1.5 copy in a 15-microliter assay system) could also be detected within a 90 min reaction time (Figure 3c). Before analyzing clinical SARS-CoV-2 RNA samples, assay selectivity was also demonstrated by challenging the detection of other respiratory disease pathogens based on the designed O-gene targeted RPA primers and crRNA (Figure 3d). The photocontrolled one-pot RNA assay was further evaluated for analysis of the O-gene from 64 clinical SARS-CoV-2 RNA samples (Figure 3e, Figure S5). Setting a cycle threshold (C_t) value of 38 as a criterion. The test results were highly consistent with a parallel reverse transcription quantitative PCR (RT-qPCR)

analysis based on a clinically approved kit, except for one PCR-confirmed positive sample and three suspected samples (C_t > 38) that were not detected (Figure 3f, and Figure S6-S8, Table S4) the obtained detection sensitivity and specificity were 99.1% and 100%, respectively (Figure 3g). It is worth noting that a more accurate comparison requires a larger sample size. This is because reproducibility is prone to fluctuation at low RNA concentrations (C_t values between 35 and 38). In addition, the difference in sample volume used in the CRISPR and PCR methods (2 L versus 2.5 L) may also contribute to the difference in test results. The photocontrolled one-pot RNA assay has been shown to achieve similar sensitivity and specificity to RT-qPCR, although further optimization is needed. Clearly, some of its advantages may be attractive for future development of more user-friendly nucleic acid testing techniques. For example, the CRISPR method is obviously faster than the PCR method. By comparative analysis of three samples with a C_t value of approximately 35, we found that the photocontrolled one-pot RNA assay could identify positive samples within 10-20 min, while the PCR method required 35 cycles (equivalent to approximately 70 min) (Figure 3h and 3i). Moreover, another seven clinical samples previously validated by RT-qPCR were detected by the photocontrolled one-pot RT-RPA-CRISPR-Cas12a assay with three different photoactivation timing (10, 20, and 30 min) (Figure S9). The results showed that setting an earlier photoactivation time will shorten the total detection time for the samples with C_t value of less than 36. Therefore, it is anticipated that the photocontrolled one-pot assay has significant potential for the rapid clinical screening of infectious disease due to the samples with C_t value > 35 are usually considered to have low infectivity.

Discussion

Thirty-eight years after its invention, PCR remains the gold-standard technique for nucleic acid testing[17]. However, large-scale infectious disease outbreaks have put new demands on nucleic acid detection techniques[8]. Future advances in nucleic acid detection technology are expected to be more sensitive, faster, more specific, and simpler. For example, one might wish that nucleic acid tests could be as simple as at-home immunoassays (such as lateral flow strips)[18]. Efforts to address these issues are ongoing. For example, the development of isothermal nucleic acid amplification technology can make nucleic acid amplification faster and simplify the amplification equipment. However, isothermal nucleic acid amplification is usually not as sensitive and specific as PCR[19]. The emergence of CRISPR technology provides a promising opportunity to solve these problems. For example, guided RNA-mediated nucleic acid recognition can overcome the problems of non-specificity, and the signal amplification mechanism of trans-cleavage of the CRISPR-Cas12 and CRISPR-Cas13 systems can improve their detection efficiency[20]. In addition, the CRISPR reaction is compatible with the temperature of isothermal nucleic acid amplification. For example, the CRISPR-Cas12a and CRISPR-Cas13a systems are temperature compatible with RPA, while the CRISPR-Cas12b system is compatible with LAMP. Based on these advantages, new nucleic acid detection methods such as SHERLOCK, DETECTOR, and HOLMES platforms have been rapidly developed.

However, these methods still lack competitive advantages when compared with PCR at the current stage. PCR can currently be performed in a closed tube, all reagents are added in one step, and the assay is run automatically. However, due to the incompatibility of nucleic acid amplification and CRISPR reactions in the SHERLOCK, DETECTOR, and HOLMES platforms, these two reactions usually need to be conducted separately. This two-step reaction complicates the detection procedure, poses a risk of contamination, and thus compromises the potential for commercial application. Single-tube CRISPR diagnostic strategies have also been developed based on some compromise designs to mitigate this incompatibility[8-10, 21]. For example, the cleavage of target nucleic acids by CRISPR reactions can be reduced by adjusting the reaction buffer[9[0] or Cas protein concentration[21a], or using less efficient PAM sites[9[a], or using phase separation solutions[10]. However, these methods compromise the efficiency of CRISPR, so these methods are often not sensitive enough for clinical detection.

We have developed a photocontrolled CRISPR diagnostic solution to solve this problem[1[1b]. As has been discussed, strategies for regulating the Cas12a reaction based on photocaleavable complementary strands and crRNA hybridization remain cumbersome. The need for careful optimization of hybridization conditions

to block crRNA is not conducive to the development of rapid, simple, and reproducible nucleic acid detection techniques. In this study, we propose a simpler scheme of directly silencing crRNA activity based on modified photocaged groups. NPOM, a photocleavable group that has been proven to be able to regulate the sgRNA of the Cas9 system, was used to
Angewandte Chemie International Edition
10.1002/anie.202300663
WILEY-VCH
RESEARCH ARTICLE
modify the crRNA of the LbCas12a system to confirm the feasibility of the photoactivated Cas12a reaction. We demonstrated that the modification of the crRNA spacer region with 3 NPOMs can completely block the activity of crRNA. This modification is very stable, and the light-mediated activity recovery is very fast (30 sec) and efficient (90.2%). In particular, the detection efficiency of the photoactivated Cas12a reaction is nearly equivalent to that of conventional unmodified crRNA, establishing a foundation for the development of a highly sensitive photocontrolled Cas12a assay. In addition, since the NPOM modification lies in the spacer region of crRNA, it will not disrupt the binding of crRNA and Cas12a. This means that Cas12a/crRNA complexes can be prepared in advance, which could be very useful for the development of lyophilized reagents in the future.

Current evidence suggests that the modification of the spacer region of crRNA with 3 NPOMs may be optimal. Modification with less NPOM does not completely block its activity, and modification with more NPOM impairs crRNA efficiency. Four crRNAs, which targeted ASFV DNA, MPXV DNA, EBV DNA, and the O-gene of SARS-CoV-2, showed excellent light-switching responses using this modification strategy. In a further study by observing 14 designed caged crRNAs indicated that discontinuous modification of the three NPOM-dts at positions 1-15 of the crRNA in the spacer region achieved excellent silencing and photoactivation efficiency, signifying that the light-start Cas12a reaction based on NPOM-modified crRNA is easy to design and extend to new targets (Figure S2). The light-start Cas12a reaction has proven to be very useful in constructing photocontrolled one-pot assays. The photocontrolled one-pot assay was demonstrated to be 50-fold more sensitive than the conventional one-pot assay. Because the light-start Cas12a reaction does not impair isothermal nucleic acid amplification efficiency, we can adjust the timing of UV irradiation to achieve faster nucleic acid detection. Comparative analysis indicated that the clinical detection of EBV and SARS-CoV-2 RNA samples by PCR required 60 to 80 min, while the detection of these same samples using the photocontrolled one-pot assay required only 10 to 20 min. Importantly, although the detection speed was significantly improved, the sensitivity was not significantly compromised. The signal-to-noise ratio obtained by detecting samples with C_i values as low as 35 is still very high. Because samples with C_i values > 35 are considered to have low infectivity, the current photocontrolled CRISPR diagnostic technique has significant potential for the rapid clinical testing of COVID-19. The test speed of 10-20 min is close to that of an athome immunoassay (approximately 10 min for a test). Because nucleic acid testing is far more sensitive than immunoassays, advances in the detection speed are important for the realization of user-friendly at-home nucleic acid diagnostics in the future. It is important to note that the new photocontrolled CRISPR diagnostic technology is simple to use. Caged crRNA can be directly chemically synthesized as regular crRNA, so the testing procedure is almost identical to the regular CRISPR diagnostics except that a 30 sec photoactivation step is applied. The fluorescence detection device equipped with a UV photoregulatory module is also very simple to build, and we are continuing to optimize the device to make it more portable (Figure S10). The practical detection capabilities of this device are also demonstrated by comparing its detection efficiency and speed with the RT-qPCR method for simultaneously measuring a clinical SARS-CoV-2 RNA sample with a C_t value of 35.76 (Supplementary movie). We expect that this advance in CRISPR diagnostics will promote widespread detection applications in biomedicine, agriculture, and food safety.

Acknowledgements

We thank Sun Yat-sen University Cancer Center for kindly providing EBV samples used in this study. This

work was supported by grants from the National Natural Science Foundation of China (32150019, 91959128, and 21874049), the Key Research and Development Plan of Hubei Province (2020BCA090), and the Basic and Applied Basic Research Foundation of Guangdong Province (2021A1515220164).
Keywords: caged crRNA · CRISPR-Cas12a · photoactivation · nucleic acid detection · one-pot assay
[1] a) J. D. Sander, J. K. Joung, Nat. Biotechnol. 2014, 32, 347-355; b) M. M. Kaminski, O. O. Abudayyeh, J. S. Gootenberg, F. Zhang, J. J. Collins, Nat. Biomed. Eng. 2021, 5, 643-656; c) G. Liu, Q. Lin, S. Jin, C. Gao, Mol. Cell 2021, 82, 333-347; d) G. J. Knott, J. A. Doudna, Science 2018, 361, 866-869
[2] a J. P. Thornhill, S. Barkati, S. Walmsley, J. Rockstroh, A. Antinori, L. B. Harrison, R. Palich, A. Nori, I. Reeves, M. S. Habibi, V. Apea, C. Boesecke, L. Vandekerckhove, M. Yakubovsky, E. Sendagorta, J. L. Blanco, E. Florence, D. Moschese, F. M. Maltez, A. Goorhuis, V. Pourcher, P. Migaud, S. Noe, C. Pintado, F. Maggi, A. E. Hansen, C. Hoffmann, J. I. Lezama, C. Mussini, A. Cattelan, K. Makofane, D. Tan, S. Nozza, J. Nemeth, M. B. Klein, C. M. Orkin, S. H.-n. C. Group, N. Engl. J. Med. 2022, 387, 679-691; b) C. Wang, P. W. Horby, F. G. Hayden, G. F. Gao, Lancet 2020, 395, 470-473.
[3] a) R. Weissleder, H. Lee, J. Ko, M. J. Pittet, Sci. Transl Med 2020, 12, eabc1931; b) M. J. Mina, K. G. Andersen, Science 2021, 371, 126-127.
[4] a) Y. Li, S. Li, J. Wang, G. Liu, Trends Biotechnol. 2019, 37, 730-743; b) M. P. Terns, Mol. Cell 2018, 72, 404-412; c) D. S. Chertow, Science 2018, 360, 381-382.
[5] J. S. Gootenberg, O. O. Abudayyeh, J. W. Lee, P. Essletzbichler, A. J. Dy, J. Joung, V. Verdine, N. Donghia, N. M. Daringer, C. A. Freije, C. Myhrvold, R. P. Bhattacharyya, J. Livny, A. Regev, E. V. Koonin, D. T. Hung, P. C. Sabeti, J. J. Collins, E. Zhang, Science 2017, 356, 438-442.
[6] J. S. Chen, E. Ma, L. B. Harrington, M. Da Costa, X. Tian, J. M. Palefsky, L. A. Doudna, Science 2018, 360, 436-439
[7] S. Y. Li, Q. X. Cheng, J. M. Wang, X. Y. Li, Z. L. Zhang, S. Gao, R. B. Cao, G. P. Zhao, J. Wang, Cell Discov. 2018, 4, 20.
[8] a) R. Wang, C. Qian, Y. Pang, M. Li, Y. Yang, H. Ma, M. Zhao, F. Qian, H. Yu, Z. Liu, T. Ni, Y. Zheng, Y. Wang, Biosens. Bioelectron. 2021, 172, 112766; b) B. Wang, R. Wang, D. Wang, J. Wu, J. Li, J. Wang, H. Liu, Y. Wang, Anal. Chem. 2019, 91, 12156-12161; c) B. Pang, J. Xu, Y. Liu, H. Peng, W. Feng, Y. Cao, J. Wu, H. Xiao, K. Pabbaraju, G. Tipples, M. A. Joyce, H. A. Saffran, D. L. Tyrrell, H. Zhang, X. C. Le. Anal. Chem. 2020, 92, 16204-16212; d) Y. Chen, Y. Shi, Y. Chen, Z. Yang, H. Wu, Z. Zhou, J. Li, J. Ping, L. He, H. Shen, Z. Chen, J. Wu, Y. Yu, Y. Zhang, H. Chen, B. Sens. Rineelectron. 2020, 169, 112642
[9] a) S. Lu, X. Tong, Y. Han, K. Zhang, Y. Zhang, Q. Chen, J. Duan, X. Lei, M. Huang, Y. Qiu, D.-Y. Zhang, X. Zhou, Y. Zhang, H. Yin, Nat. Biomed. Eng. 2022, 6, 286-297; b) J. Arizti-Sanz, C. A. Freije, A. C. Stanton, B. A. Petros, C. K. Boehm, S. Siddiqui, B. M. Shaw, G. Adams, T. F. Kosoko-Thoroddsen, M. E. Kemball, J. N. Uwanibe, F. V. Ajogbasile, P. E. Eromon, R. Gross, L. Wronka, K. Caviness, L. E. Hensley, N. H. Bergman, B. L. MacInnis, C. T. Happi, J. E. Lemieux, P. C. Sabeti, C. Myhrold, Nat. Commun. 2020, 11. 5921
[10] a) K. Yin, X. Ding, Z. Li, H. Zhao, K. Cooper, C. Liu, Anal. Chem. 2020, 92, 8561-8568; b) M. Lin, H. Yue, T. Tian, E. Xiong, D. Zhu, Y. Jiang, X. Zhou, Anal. Chem. 2022, 94, 8277-8284.
[11] a) Y. Chen, X. Xu, J. Wang, Y. Zhang, W. Zeng, Y. Liu, X. Zhang, Anal. Chem. 2022, 94, 9724-9731; b) M. Hu, Z. Qiu, Z. Bi, T. Tian, Y. Jiang, X. Zhou, Proc. Natl. Acad. Sci. U.S.A. 2022, 119, e2202034119.
[12] a) Y. Liu, R. S. Zou, S. He, Y. Nihongaki, X. Li, S. Razavi, B. Wu, T. Ha, Science 2020, 368, 1265-1269; b) E. V. Moroz-Omori, D. Satyapertiwi, M. C. Ramel, H. Hogset, I. K. Sunyoszki, Z. Liu, J. P. Wojciechowski, Y. Zhang, C. L. Grigsby, L. Brito, L. Bugeon, M. J. Dallman, M. M. Stevens, ACS Cent. Sci. 2020, 6, 695-703; c) W. Y. Zhou, W. Brown, A. Bardhan, M. Delaney, A. S. Ilk, R. R. Rauen, S. I. Kahn, M. Tsang, A. Deiters, Angew. Chem. Int. Ed. 2020, 59, 8998-9003; d) Y. Wang, Y. Liu, F. Xie, J. Lin, L. Xu, Chem. Sci. 2020, 11, 11478-11484.
[13] H. Lusic, D. D. Young, M. O. Lively, A. Deitors, Org. Lett. 2007, 9, 1903-1906.

10.1002/anie.202300663

[14] O. Piepenburg, C. H. Williams, D. L. Stemple, N. A. Armes, PLOS Biol. 2006, 4, 1115-1121.
[15] a) J. I. Cohen, N. Engl. J. Med. 2000, 343, 481-492; b) L. S. Young, A. B. Rickinson, Nat. Rev. Cancer 2004, 4, 757-768.
[16] a) K. C. A. Chan, J. K. S. Woo, A. King, B. C. Y. Zee, W. K. J. Lam, S. L. Chan, S. W. I. Chu, C. Mak, I. O. L. Tse, S. Y. M. Leung, G. Chan, E. P. Hui, B. B. Y. Ma, R. W. K. Chiu, S. F. Leung, A. C. van Hasselt, A. T. C. Chan, Y. M. D. Lo, N. Engl. J. Med. 2017, 377, 513-522; b) P. Busson, C. Keryer, T. Ooka, M. Corbex, Trends Microbiol. 2004, 12, 356-360.
[17] K. Mullis, F. Faloona, S. Scharf, R. Saiki, G. Horn, H. Erlich, Cold Spring, Harb. Symp. Quant. Biol. 1986, 51, 263-273.
[18] A. McDermott, Proc. Natl. Acad. Sci. U.S.A. 2020, 117, 25956-25959.
[19] J. C. Rolando, E. Jue, J. T. Barlow, R. F. Ismagilov, Nucleic Acids Res. 2020, 48, e42.
[20] a) D. C. Swarts, M. Jinek, Mol. Cell 2019, 73, 589-600; b) A. East-Seletsky, M. R. O'Connell, S. C. Knight, D. Burstein, J. H. Cate, R. Tjian, J. A. Doudna, Nature 2016, 538, 270-273; c) B. Tian, G. A. S. Minero, J. Fock, M. Dufva, M. F. Hansen, Nucleic Acids Res. 2020, 48, e30; d) S. Y. Li, Q. X. Cheng, J. K. Liu, X. Q. Nie, G. P. Zhao, J. Wang, Cell Res. 2018, 28, 491-493.
[21] a) Y. Chen, Y. Mei, X. Zhao, X. Jiang, Anal. Chem. 2020, 92, 14846-14852; b) X. Ding, K. Yin, Z. Li, R. V. Lalla, E. Ballesteros, M. M. Sfeir, C. Liu, Nat. Commun. 2020, 11, 4711.
Angewandte Chemie International Edition
10.1002/anie.202300663
WILEY-VCH
RESEARCH ARTICLE
Entry for the Table of Contents
![Photocontroled one-pot assay\n1 RPA\nGenome DNA\nRT-RPA\nd1DNA\n2\nLight\n](5/eeSnBYxHk3lOr6r5YK0awH/pdf_d52a49c73ca3df75afa97d4b293af708_b10e0519888df524f7b5ce37d594b1ef7508518051523035/tmp_zip_img/9e1d004d-77ce-43e9-a35f-d16c8c5df5da.png)
A robust photocontrolled one-pot assay was developed by combining a light-start CRISPR-Cas12a reaction system and recombinase polymerase amplification (RPA) for nucleic acid detection. With this platform, the clinical samples of Epstein-Barr virus and severe acute respiratory syndrome coronavirus 2 (SARS-CoV-2) samples can be effectively detected.